Multiple beats of weakly confined excitons with inverted selection rule

Hideki Yasuda and Hajime Ishihara*
Department of Physics and Electronics, Osaka Prefecture University, Sakai 599-8531, Japan
(Received 16 February 2009; published 18 May 2009)

The phenomenon of multiple beats (MBs) arising from nondipole-type excitons weakly confined in a thin film is theoretically elucidated using a nonlocal transient-response theory. Kojima *et al.* previously demonstrated for a GaAs thin film that the degenerate four-wave mixing signals from the quantized levels of the center-of-mass motion of excitons exhibit complex interference between beats under femtosecond-order pulse incidence [Kojima *et al.*, J. Phys. Soc. Jpn. **77**, 044701 (2008)]. This leads to an ultrafast optical response on the order of femtoseconds. This effect occurs in a size region beyond the long-wavelength approximation regime due to the resonant enhancement of the internal field, wherein the usual dipole selection rule is violated. Our analysis of MBs employs a model of the nonlocal multilevel system that considers the spatial interplay between excitonic waves and the radiation field to elucidate the mechanism behind the observed ultrafast response.

DOI: 10.1103/PhysRevB.79.193308 PACS number(s): 71.35.−y, 71.36.+c, 78.67.−n, 82.53.Mj

The combination of ultrafast laser techniques and nanofabrication technology has opened new possibilities for high-performance control over nonlinear optical response. This can be achieved through the interference of induced polarizations from multiple quantized levels. Coherent interference phenomena, i.e., beating effects have been observed in various systems, e.g., the interference between heavy and light hole excitons,[1] upper and lower polaritons,[2] and confined excitons in quantum wells.[3] In addition, the control of the dynamics of the response signal using this interference has been demonstrated. In particular, this method allows considerable control over signal decay allowing the possibility for high-speed signal processing.

Recently, peculiar size-dependent nonlinearity for excitons with center-of-mass (c.m.) confinement has been observed, which further increases the number of degrees of freedom that can be used to control optical response. Motivated by the theoretical proposal,[4] it was demonstrated that a large nonlinearity results from the size-resonant enhancement of the internal field for the size region beyond long-wavelength approximation (LWA),[5,6] wherein the usual dipole selection rule is violated and the nondipole-type states of the excitonic c.m. motion significantly contribute to the optical response. By using this type of nonlinear process, more recently, femtosecond-order response has been demonstrated by the simultaneous excitation of multiple c.m. excitonic levels with a spectrally broad incident pulse,[7] where the multiple beats (MBs) between the different c.m. levels generated by degenerate four-wave mixing (DFWM) strongly affects the time profile of the response signal. The superposition of these MBs has been attributed to a significant shortening of the response signal. This mechanism has potential in ultrafast signal processing because of the considerably large nonlinearity created by the resonant field enhancement and also because of the high level of controllability over the excitonic level scheme allowed by appropriate nanostructure design. However, this has not been fully explored because of the difficulties involved in analyzing the transient response in the non-LWA regime, where the microscopic spatial interplay between excitonic and radiation waves plays a key role. In this Brief Report, therefore, we theoretically elucidate the dynamics of the MBs of a c.m.-confined excitonic system in the non-LWA regime. Especially, we present an analysis of the experimental results in Ref. 7 employing a nonlocal transient-response theory developed by us.

Figure 1(a) shows a schematic picture of the sample used in Ref. 7 with double heterostructures consisting of three GaAs layers with a thickness of about $X=110$ nm. Among the three active layers, the topmost, having the highest quality, provides the dominant response signal.[6] Therefore, in our calculation, we simplify the model as shown in Fig. 1(b), namely, we consider a single layer corresponding to the topmost as an excitonic active layer and the other part of the sample is treated as a material with only the background dielectric constant ε_b of GaAs. The difference in background dielectric constant between GaAs and AlGaAs is not essential in the present study.

As a model for excitons, we consider the excitonic c.m. motion being confined in a thin layer with its thickness directed along the z axis. Since the excitonic Bohr radius is large for GaAs (14 nm), the distortion of the c.m. wave function should be considered in the form of a dead-layer model[8] or transition-layer model.[9] In the present study, this effect is considered as a change in effective thickness and we explicitly treat only the degree of freedom of c.m. motion. Within

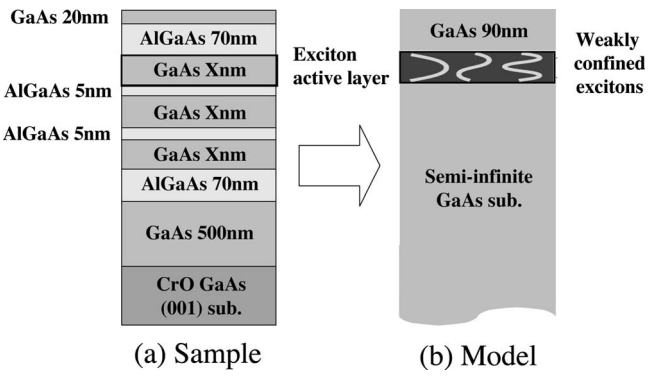

FIG. 1. (a) Experimental sample consisting of three GaAs layers. (b) Theoretical model of a sample. The wavy lines represent the excitonic c.m. wave functions.

the subspace of a given wave vector parallel to the film surface, $K_{\parallel}$, we consider the following eigenfunctions and eigenenergies as the basis of the c.m. motion of excitons along the z axis: $\psi_n(\mathbf{z})=(2/d)^{1/2}\sin K_n z$ and $E_n=\hbar^2(K_n^2+K_{\parallel}^2)/2M$, where d is the active-layer thickness, M is the effective mass of the exciton, and K_n is the quantized wave number perpendicular to the film surface and whose quantization condition is given as $K_n=n\pi/d$ for a positive integer n.

In the calculation of the linear response, we consider the nonlocal relationship between the induced polarization $P(z)$ and the electric field $E(z)$ along with the method in Ref. 10. The induced polarization can be expanded as $P(z)=\Sigma_n X_n(\omega)\psi_n(z)$ with the bases of excitonic c.m. motion.[10] The spectrum of the expansion coefficient $|X_n(\omega)|^2$ includes information on the radiative shift and width of the nth excitonic state.

As for the origins of this nonlinearity, we consider involvement of the state filling due to Pauli's exclusion effect and the exciton-exciton interaction. Discretizing the medium and assuming one-dimensional transfer reduced from the effective mass M, we introduced an attractive interaction between the excitons at neighboring sites, which yields a biexicton and free two-exciton states. In the considered effect, however, the contributions from the two-exciton states are not significant and actually, their explicit effects are not found in the basic results of the experiment. Therefore, in the present study, we focus on the effects of one-exciton resonance due to the state filling.

To calculate the DFWM signal, we use the Runge-Kutta method to numerically solve as functions of time t the simultaneous equations of motion of the density matrix

$$\dot{\rho}_{mn}=\frac{i}{\hbar}(\epsilon_m-\epsilon_n)\rho_{mn}-\Gamma_{mn}\rho_{mn}+\frac{i}{c\hbar}\left[\sum_l\left\{\rho_{lm}\int\langle n|\hat{\boldsymbol{J}}(z)|l\rangle\boldsymbol{A}(z,t)dz-\rho_{nl}\int\langle l|\hat{\boldsymbol{J}}(z)|m\rangle\boldsymbol{A}(z,t)dz\right\}\right] \quad (1)$$

and the standard Maxwell equation to describe the vector potential $\mathbf{A}(z,t)$, written in the Coulomb gauge. In the above expression, $\{\epsilon_n\}$ denotes the eigenenergies of the states $\{|n\rangle\}$, and Γ_{mn} is the phenomenologically introduced nonradiative damping constant. The Maxwell equation includes the source current density $\boldsymbol{j}(z,t)$, which is the quantum-mechanical average of the current-density operator $\hat{\boldsymbol{J}}(z)$, that is, $\boldsymbol{j}(z,t)=\Sigma_{nm}\rho_{mn}\langle n|\hat{\boldsymbol{J}}(\boldsymbol{r})|m\rangle$. In this calculation, we do not neglect the microscopic position dependence of $\boldsymbol{A}(z,t)$ and $\boldsymbol{j}(z,t)$ to properly include the contributions from the higher order $(n\geq 2)$ of excitonic states beyond the LWA regime. From the solution of $\boldsymbol{A}(z,t)$ obtained by assuming negligibly small $K_{\parallel}$, we extract the component of the DFWM signal corresponding to the observed signal by the numerical technique. Further, Fourier transformation of the calculated signals affords the DFWM spectrum. Because of the self-consistent treatment of $\boldsymbol{A}(z,t)[\boldsymbol{E}(z,t)]$ and $\boldsymbol{j}(z,t)[\boldsymbol{P}(z,t)]$ in the above calculations, the size-dependent radiative correction (shift and width) or radiative decay-time profile automatically appears in the result. Note that the only fitting parameters in the present calculation are d and Γ.

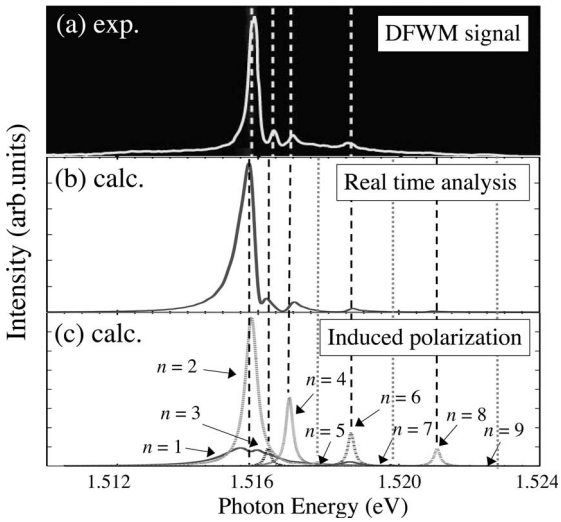

FIG. 2. (a) Observed DFWM spectrum in a GaAs thin film. (b) DFWM spectrum obtained by Fourier transformation of the signal calculated by the real time analysis. (c) Calculated induced polarization spectra. The nonradiative damping constants are assumed to be $\Gamma_{10}=0.6$ meV, $\Gamma_{k0}=0.1$ meV $(k=2,3,\ldots,N)$.

Figure 2(a) shows the DFWM spectrum experimentally observed by a (Gaussian-shaped) pulse excitation with a duration of 170 fs and with no delay between the pump and the probe pulses.[7] Also shown is the calculated DFWM spectrum and those of the components of the polarization induced by the individual c.m. states $|X_n(\omega)|^2$ in Figs. 2(b) and 2(c), respectively. We find that the peak energy of each component of the observed DFWM spectrum is in good accordance with that of $|X_n(\omega)|^2$. In the present sample, the peak at $n=1$ almost overlaps that at $n=2$, which is due to the large radiative shift at $n=1$. In this fitting, we find that the signal intensities from the excitonic states with even parity $(n=2,4,6,\ldots)$ are prominent while those from the excitonic states with odd parity are weak except for that at $n=1$. This inversion of selection rule is principally due to the nanoscale spatial structure of the internal field. Further, this spectral shape is very sensitive to the nonradiative damping constants of the respective c.m. states. In this fitting, we chose the following combination: $\Gamma_{10}=0.6$ meV, $\Gamma_{k0}=0.1$ meV $(k=2,3,\ldots,N)$. It should be noted that Γ_{10} is considerably large; this enhances the character of the inverted selection rule in this sample.

The experimentally observed DFWM intensities are plotted as functions of delay time[7] in Fig. 3. For this measurement, a series of the square-shaped pulses were generated by a pulse-processing system composed of a slit and grating pair, which allowed the selection of a particular group of c.m. states that would be excited. In Fig. 3(a), the spectral width of square-shaped pulse ΔE is gradually widened while in Fig. 3(b), each square-shaped pulse had a constant spectral width of $\Delta E=5.4$ meV and its center energy was finely adjusted to increase, one by one, the number of involved exci-

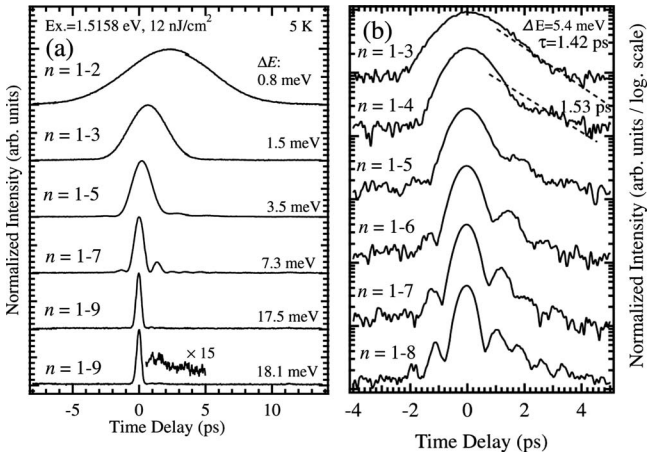

FIG. 3. (a) Observed DFWM intensities as functions of delay time for different incident pulse widths. (b) Observed excitation-energy dependence of DFWM signal (Ref. 7).

tonic states within the square-shaped pulses.[7] The involved states are indicated for each curve. We observe two characteristic behaviors through these figures. One is the shortening of the response pulse with an increase in the spectral pulse width [Fig. 3(a)] and the other is the discrete change in the oscillatory structure to a sharp, more undulating shape with an increasing number of included excitonic states [Fig. 3(b)]. These characteristic behaviors are explained qualitatively in terms of the superposition of MBs in Ref. 7. However, a full understanding of the origin of these effects should be obtained from microscopic theory to reproduce the signals from the nonlocal response system.

Before discussing the decay behavior of the DFWM signals using a full nonlocal calculation, we examined how the superposition of MBs contributing to the shortening of the response signal by using a simple analytical calculation. With use of the perturbative expansion and the rotating-wave approximations, we derive the expression of the output pulse energy for DFWM from Eq. (1) by extending the method of Yajima and Taira[11] for the two-level system to the N-level nonlocal system. The incident pulse is assumed to be of delta-function type to perform an analytical calculation. We obtain

$$J_{\mathrm{DFWM}}^{(3)}(\tau) = \frac{1}{2}\sum_{k=1}^{N}\frac{\hbar}{\Gamma_{k0}}\Bigg[J(k)^2 e^{-2\Gamma_{k0}/\hbar\tau} + \sum_{k'(\neq k)=1}^{N} I(k,k')^2 e^{-2\Gamma_{k'0}/\hbar\tau} + 2J(k)\sum_{k'(\neq k)=1}^{N} I(k,k') e^{-(\Gamma_{k'0}/\hbar+\Gamma_{k0}/\hbar+i\omega_{kk'})\tau}\Bigg], \tag{2}$$

where $\tau(\geq 0)$ is the delay time between the pump and the probe pulses, $\omega_{k'k}=\epsilon_{k'}/\hbar-\epsilon_k/\hbar$, and $J(k)$ and $I(k,k')$ include overlap integrals between the light wave and the respective excitonic waves. The third term on the right-hand side (RHS) of Eq. (2) represents the multiple interference among the N excitonic states through the third-order interaction.

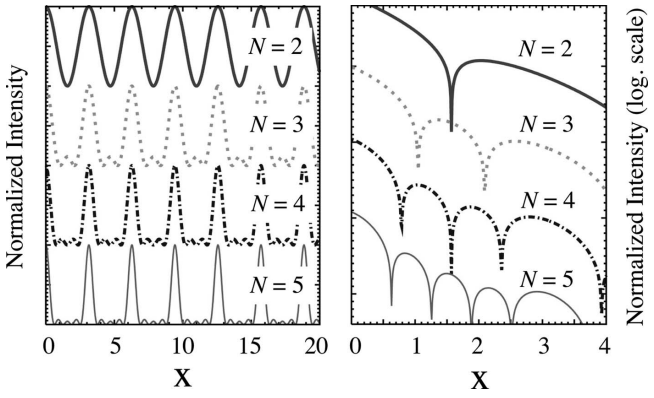

FIG. 4. Calculated examples of function $M(x)$ for $N=2-5$. (a) $\Gamma_{10}/\hbar=\Gamma_{k0}/\hbar=0$. (b) $\Gamma_{10}/\hbar=\Gamma_{k0}/\hbar=1$ $(k=2\sim N)$.

Taking the term for $k=1$ in the square bracket on the RHS of Eq. (2) because of symmetry, we obtain

$$M(\tau) = e^{-2\Gamma_{10}/\hbar\tau} + \sum_{k=2}^{N} e^{-2\Gamma_{k0}/\hbar\tau} + 2\sum_{k=2}^{N} e^{-(\Gamma_{10}/\hbar+\Gamma_{k0}/\hbar+i\omega_{1k})\tau}, \tag{3}$$

where we take $J(k)=I(k,k')=1$ for the simplified demonstration.

Further, for simplicity, we assume a constant energy spacing between the neighboring states, δE, that is, $\hbar\omega_{1k'}=\delta E_{1k'}=(k'-1)\delta E$ $(k'=2,3,\ldots)$. In this case, the third term on the RHS can be rewritten as

$$\frac{\sin Nx}{\sin x}\cos(N-1)x - 1 \quad \left(x=\frac{\delta E}{2\hbar}\tau\right) \tag{4}$$

if we assume the damping constants to be zero.

Figure 4(a) shows some examples of the function $M(x)$ for $N=2-5$. As seen in this figure, the shortening of the response signal can be attributed to the superposition of MBs, as explained in Ref. 7. Similar shortening due to MBs has been discussed for various multilevel systems.[12,13] Furthermore, if we assume finite damping constants and plot on a logarithmic scale, a decay profile similar to that observed is obtained along with similar discrete changes in the beat oscillation [Fig. 4(b)].

The above examination provides a basic insight into the mechanism behind the observed phenomenon. However, the real phenomenon is greatly affected by the incident pulse shape and the damping constants. Thus, we now turn to the results of the nonlocal transient-response calculation to gain a full understanding of the phenomenon. Figure 5 shows the calculated results, where both panels (a) and (b) match very well with the results in Fig. 3. However, in this demonstration, we have made a special consideration on the damping constants and the incident pulse shape. For the present fitting, the damping constants increased when a higher excitation energy was used (see caption to Fig. 5.) The slow decay of curve A in Figs. 5(a) and 5(b) can be reproduced if we assume a considerably small damping constant of at least

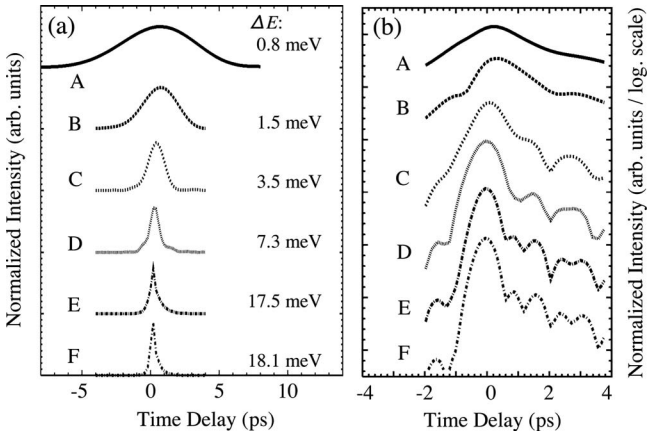

FIG. 5. (a) Calculated DFWM intensities as functions of delay time for different incident pulse widths, and (b) excitation-energy dependence of DFWM signals calculated by real time analysis. We identify the beating structure of curves A and B for $N=2$ in Fig. 4(b), C and D for $N=3$, and E and F for $N=4$. The assumed damping constants are for curves A, B, C, D, E, and F, respectively, are as follows: (a) 0.15, 0.30, 0.40, 0.40, 0.40, and 0.60 meV; and (b) 0.10, 0.20, 0.30, 0.30, 0.35, and 0.40 meV.

that in the $n=1$ state. However, the short response signal and beating behavior of curve F in Figs. 5(a) and 5(b), respectively, requires a large damping constant of at least that in the $n=1$ state. But, if the damping constant in the $n=1$ state is as small as that for curve A, the beating behavior cannot be reproduced. The larger damping for the excitation of the higher-energy region is reasonable because the larger component of the band excitation introduces the higher carrier density that causes the larger dephasing.[14] Further, this beating behavior is not reproduced if we assume an even-weighted excitation of all the involved c.m. levels. But clear beating appears if we assume weaker excitation of the lower state $(n=1)$ by considering the distortion of the square-shaped pulses on the lower-energy side.[15] By observing the above two elements, we understand that the experimentally observed shortening of the response signal and the discrete change in the beats with the excitation-energy range is due to not only to MBs but also to the fast dephasing in the $n=1$ state, which enhances the character of the inverted selection rule of the present system.

In summary, we investigated the effect of multiple interference in DFWM by c.m.-confined states. The observed discrete transition of the oscillating behavior and shortening of the response signal is accurately reproduced by our nonlocal transient-response theory, where the interplay between the excitonic and radiation waves is fully considered. The scenario based on MBs proposed in Ref. 7 is elucidated by our simple analysis. However, examination of the effects of the damping constants of the respective c.m. states and the incident pulse shape revealed that the observed first response is due to not only to MBs but also the fast dephasing in the $n=1$ state caused by excitation to a higher-energy region, which enhances the character of the inverted selection rule of the present system.

The authors are grateful to T. Isu and O. Kojima for the useful information on their experiments and for the fruitful discussions.

*ishi@pe.osakafu-u.ac.jp

[1] B. F. Feuerbacher, J. Kuhl, R. Eccleston, and K. Ploog, Solid State Commun. **74**, 1279 (1990).
[2] T. Mita and N. Nagasawa, Solid State Commun. **44**, 1003 (1982).
[3] E. O. Göbel, K. Leo, T. C. Damen, J. Shah, S. Schmitt-Rink, W. Schäfer, J. F. Möller, and K. Köhler, Phys. Rev. Lett. **64**, 1801 (1990).
[4] H. Ishihara and K. Cho, Phys. Rev. B **53**, 15823 (1996).
[5] K. Akiyama, N. Tomita, Y. Nomura, and T. Isu, Appl. Phys. Lett. **75**, 475 (1999).
[6] H. Ishihara, K. Cho, K. Akiyama, N. Tomita, Y. Nomura, and T. Isu, Phys. Rev. Lett. **89**, 017402 (2002).
[7] O. Kojima, T. Isu, J. Ishi-Hayase, A. Kanno, R. Katouf, M. Sasaki, and M. Tsuchiya, J. Phys. Soc. Jpn. **77**, 044701 (2008).
[8] J. J. Hopfield and D. G. Thomas, Phys. Rev. **132**, 563 (1963).
[9] A. D'Andrea and R. Del Sole, Phys. Rev. B **25**, 3714 (1982).
[10] H. Ishihara, J. Kishimoto, and K. Sugihara, J. Lumin. **108**, 343 (2004).
[11] T. Yajima and Y. Taira, J. Phys. Soc. Jpn. **47**, 1620 (1979).
[12] C. Leichtle, I. Sh. Averbukh, and W. P. Schleich, Phys. Rev. Lett. **77**, 3999 (1996).
[13] J. Feldmann, T. Meier, G. von Plessen, M. Koch, E. O. Göbel, P. Thomas, G. Bacher, C. Hartmann, H. Schweizer, W. Schäfer, and H. Nickel, Phys. Rev. Lett. **70**, 3027 (1993).
[14] H. Wang, K. Ferrio, D. G. Steel, Y. Z. Hu, R. Binder, and S. W. Koch, Phys. Rev. Lett. **71**, 1261 (1993).
[15] If we consider further distortion independently for the probe pulse, we can also reproduce a similar behavior to the beating in the negative delay-time region. A detailed study on this point will be presented in a future publication.